Experimental Mechanics (2006) 46: 163–171
DOI 10.1007/s11340-006-6423-7

Spontaneous Mixed-Mode Fracture in Bonded Similar and Dissimilar Materials

K. Xia · V.B. Chalivendra · A.J. Rosakis

Received: 30 June 2005 / Accepted: 29 November 2005

Abstract In this paper, we report on an experimental study of spontaneous, mixed-mode, crack propagation in weakly bonded similar and dissimilar materials. A unique experimental configuration is proposed to induce spontaneous crack growth events along the interfaces. The cracks nucleate from tiny circular holes and are triggered by an exploding wire. They subsequently propagate under the action of a constant, far-field load. Dynamic photoelasticity in conjunction with high speed photography is used to capture the real-time isochromatics associated with crack propagation. In the case of identical materials, crack propagation is anti-symmetric with respect to the crack nucleation point while strong asymmetry is observed for the case of dissimilar materials. In both cases, cracks propagate at constant velocity from the initiation point. The time histories of dynamic stress intensity factors and of energy release rates of the propagating cracks along the bonded similar materials are also reported.

K. Xia (SEM member)
Department of Civil Engineering & Lassonde Institute,
University of Toronto, Toronto, Canada M5S 1A4

V. B. Chalivendra (SEM member)
Mechanical Engineering Department,
University of Massachusetts Dartmouth,
North Dartmouth, MA 02747, USA

A. J. Rosakis (✉, SEM member)
Graduate Aeronautical Laboratories,
California Institute of Technology,
Pasadena, CA 91125, USA
e-mail: rosakis@aero.caltech.edu

Keywords Bonded materials · Spontaneous dynamic fracture · Mixed-mode dynamic photoelasticity · High speed photography · Dynamic stress intensity factors · Energy release rates

Introduction

All of the experimental studies reported so far in the open literature involve dynamic crack propagation in specimens of either homogeneous materials or bonded solids which contain pre-existing cracks. In most of these studies, the pre-existing cracks are subjected to stress wave loading whose function is to initiate and sustain crack growth at various speeds. Ravi-Chandar and Knauss [1–4] studied a mode-I crack propagation problem using a transient crack face loading configuration. Another example of this is discussed by Ravichandran and Clifton [5], who studied mode-I crack propagation in a pre-cracked homogeneous material subjected to plane wave loading. Using the same idea as Ravi-Chandar and Knauss [1–4], Washabaugh and Knauss [6] investigated the limiting crack speed of mode-I cracks propagating along an interfaces between weakly bonded plates. They found that as the strength of the interface drops to zero, the crack speed approaches the theoretical limiting speed for mode-I fracture, i.e., the Rayleigh wave speed of the material. Rosakis, Shukla and their co-workers [7–10] studied crack propagation along bonded (coherent) interfaces between dissimilar materials using dynamic shear loading induced by asymmetric projectile impact. For dissimilar material systems, they found that the resulting shear cracks could propagate at speeds faster than the dilatational wave speed of the slower wave

speed constituent material, often becoming "supersonic" with respect to one side [11]. For similar material systems however, Rosakis et al. [12] found that shear cracks propagating along weak interfaces could grow at a speed faster than the shear wave speed of the material and they often approached the longitudinal wave speed for large enough loading or small enough bond strengths. Such cracks were called "supershear".

There are no experimental studies reported in the literature studying spontaneous crack growth processes, which occur in the presence of quasi-static pre-existing loading and featuring crack growth from a zero initial length. There are a few important reasons that motivate the experimental investigation of spontaneous mixed-mode crack growth subjected to far-field loading. First of all, there are many practical examples involving spontaneous fracture and catastrophic failure of civic and defense structures. Such examples involve defects of initial sizes that are often negligible compared to a whole structure, which is subjected to quasi-static tensile loading. Secondly, most of the modern engineering materials, such as fiber-reinforced composites, graded and bonded materials and structures, have interfaces which are either coherent (have intrinsic strength and toughness) or incoherent (are either damaged or have frictional strength). Since interfaces are usually weaker than the constituent materials, their spontaneous interface failure is the dominant failure mechanism in such solids [13]. Indeed, any defects in such interfaces can ultimately serve as sites of catastrophic failure nucleation during the service life of the structure. Moreover, all experimental studies on dynamic crack propagation reported so far consider either purely mode-I or predominantly mode-II conditions as discussed above. Very few studies have been reported on mixed-mode crack growth along weak planes [14, 15]. Moreover, the spontaneous mixed-mode crack propagation parameter histories such as crack propagation velocities, stress intensity factors and energy release rates for bonded interfaces have not yet been investigated, though the understanding of these issues is vital in the design of most engineering structures.

Motivated by above issues, a novel experimental technique is designed and developed to induce spontaneous mixed-mode crack growth in both bonded identical and dissimilar plates. In order to simulate spontaneous fracture, an exploding wire technique is used to initiate fracture from a very small hole in the specimen. Far-field tensile loading is used to drive the subsequent dynamic crack propagation following crack nucleation. Dynamic photoelasticity in conjunction with high-speed photography is used to capture real-time isochromatic fringe patterns associated with the entire event. These fringe patterns are later analyzed for crack tip position and crack propagation velocities. For bonded similar plates, a nonlinear least-square method is used to determine dynamic mode-I and mode-II stress intensity factors, mode mixities and dynamic energy release rates from the isochromatic fringes. For bonded dissimilar plates, asymmetry of the stress field with respect to the point of crack nucleation is duly discussed.

Experimental Details

Two different birefringent materials, Homalite-100 and polycarbonate (9.5 mm in thickness) are used in this study. The material properties are listed in Table 1. The wave speeds are measured using ultrasonics while the rest of the properties are taken from the literature [16]. The dimensions of the specimens are 150 mm × 150 mm. For bonded similar or dissimilar materials, two equally-sized plates of 150 mm × 75 mm each are used. Before bonding the two halves of the specimen, a small groove of 1 mm in width is made on the bonding interface of one of the two 150 mm × 75 mm plate along the thickness direction. A thin wire of 0.1 mm in diameter is placed in the small groove of sheet and two plates are bonded together using adhesive. Two different adhesives namely Loctite E-120HP (strong adhesive) and HARDMAN five minute epoxy (weak adhesive) are used to achieve different speeds. The average thickness of the adhesive is around 100 μm. The static mode-I fracture toughness values of these adhesives (Loctite E-120HP and HARDMAN) when glued to two polycarbonate sheets are 0.94 MPa-$m^{1/2}$ and 0.46 MPa-$m^{1/2}$ respectively. Single edge notch specimen configuration was used to obtain these static fracture toughness values. Figure 1(a) shows the experimental set-up used in this study. It consists of a laser light source, a set of circular polarizer sheets, a high speed camera, and an explosion box. A collimated beam is used to illuminate the specimen, which is

Table 1 Summary of optical and dynamic mechanical properties of photoelastic materials

Material Property	Homalite-100	Polycarbonate
Young's modulus E (MPa)	3860	2480
Poisson's ratio ν	0.35	0.38
Stress fringe value f_σ (kN/m)	23.6	7.0
P Wave speed C_P (km/s)	2.104	1.724
S Wave speed C_S (km/s)	1.200	0.960
Density ρ (kg/m^3)	1230	1192

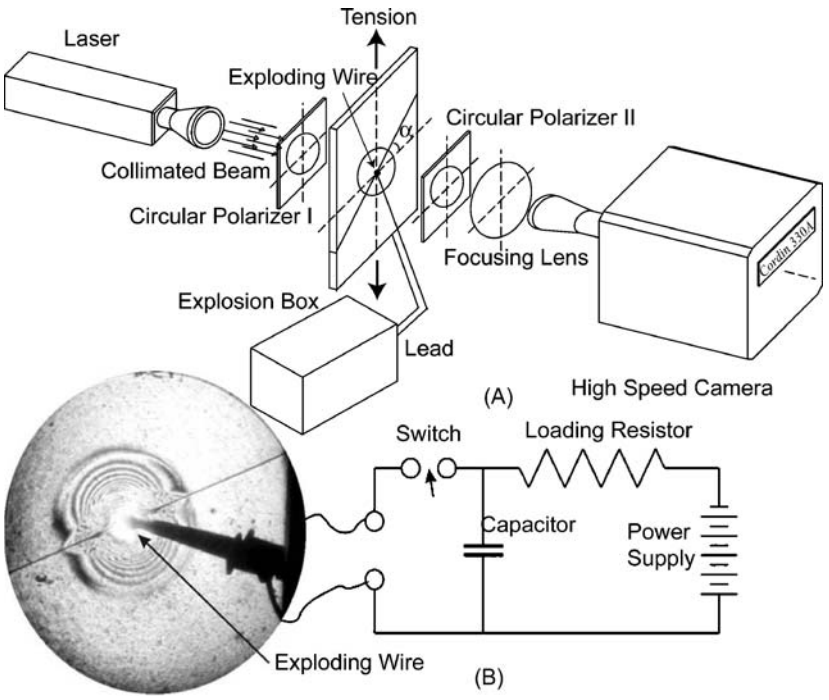

Fig. 1. Experimental setup and schematics of exploding wire circuit

sandwiched between the two circular polarizer sheets. The explosion box provides the electric energy to explode the wire, which is the critical part of the design of this spontaneous fracture configuration. The details of the explosion box were duly discussed in a previous paper [17]. The electronic explosion results in an expanding plasma wave. For the bonded specimen, this explosion creates a small crack along the interface if the toughness of the adhesive is much lower than that of the material. Under large enough static far-field loading, this initial small crack is unstable and will propagate. Upon sending the high electric energy in to the exploding wire, the explosion box also sends a triggering signal to the high speed camera. The camera system (Cordin 220) is able to capture the images at a framing rate of 100 million frames per second with exposure times as low as 10 nanoseconds. In this study, the high speed camera is operated at a much slower speed, around 0.2–0.4 million frames per second. Figure 1(b) shows the photograph of an isochromatic fringe pattern generated by an explosion at an incoherent interface between two plates. A specially designed tensile fixture is used to obtain static far-field loads.

Experimental Results of Spontaneous Fractures Along Bonded Similar Materials

A series of experiments was performed to observe the spontaneous mixed-mode crack propagation phenomenon along the bonded polycarbonate plates. In this study, three different inclination angles of interfaces, namely $\alpha = 30°$, 35°, 40° are considered. A typical photoelastic fringe pattern (isochromatics) of the specimen ($\alpha = 35°$) a few microseconds after initiation of the explosion is shown in Fig. 2. The explosion initiation point, the few isochomatic fringes associated with far-field tensile loading and the fringes generated upon nucleation of the crack at the explosion point are indicated in the figure. In analyzing the experiments, the fringe numbers of the isochromatics associated with the static far-field tensile loading before the explosion are counted. These fringe numbers are later used in analyzing the fringes of the propagating crack tip and for determining fracture parameters such as mode-I, mode-II stress intensity factors and energy release rates. As is obvious from Fig. 2 that the crack tips associated with small amounts of crack growth are obscured by the plasma generated by the explosion.

Isochromatic Fringe Patterns

A set of isochromatic fringe patterns for all three cases of $\alpha = 30°$, 35°, and 40° as is shown in Fig. 3. For each case, images corresponding to two crack lengths are displayed. The far-field tensile load applied in all three cases is 8 MPa. Loctite E-120HP (strong adhesive) is used to bond the two halves of the polycarbonate plates. Upon nucleation, the crack propagates along both directions opposite to the center of the specimen.

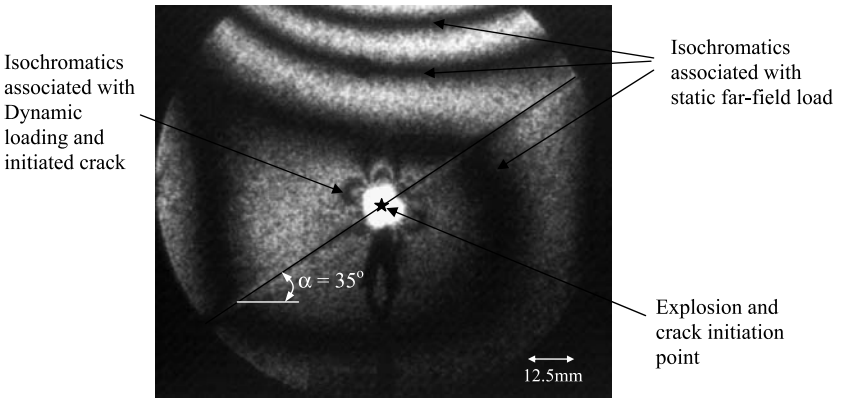

Fig. 2. Photoelastic fringe pattern of far-field loaded specimen upon initiation of the explosion

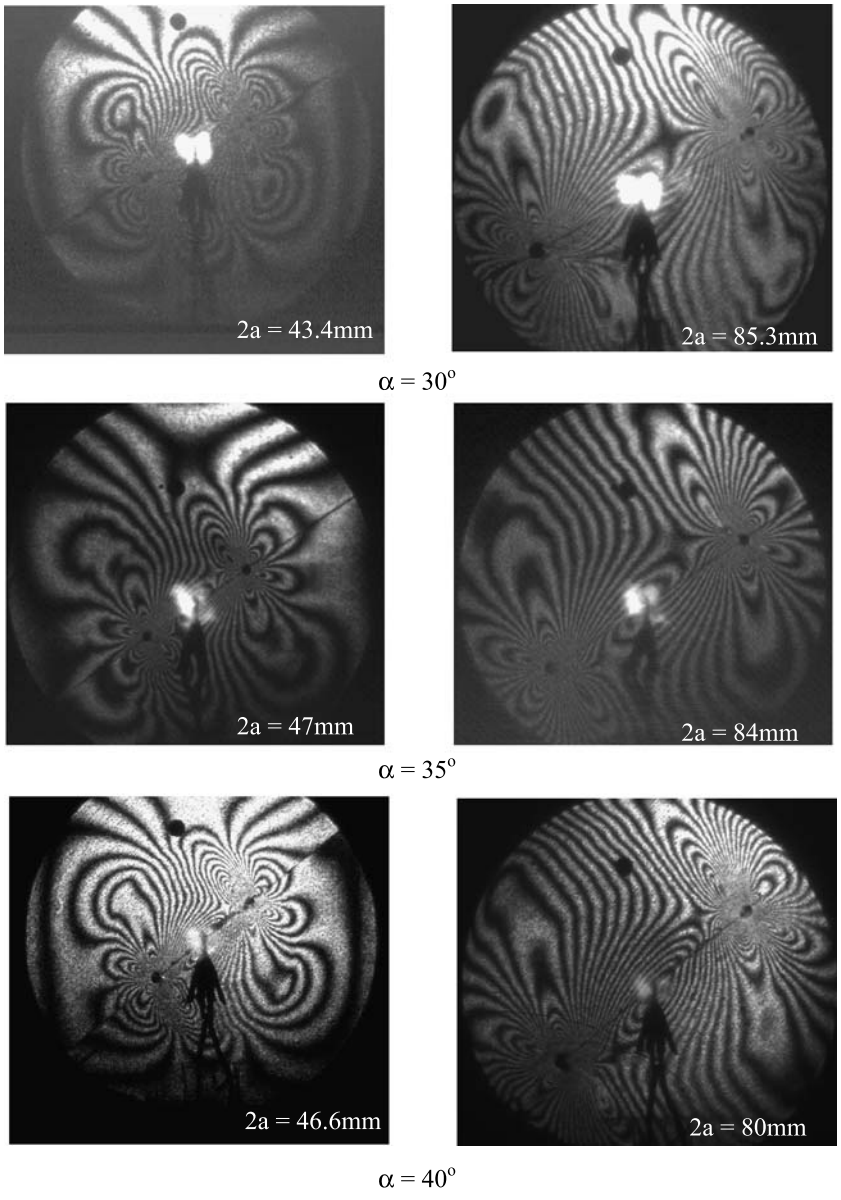

Fig. 3. Isochromatic fringe pattern associated with crack propagation along inclined planes of three different inclination angles (Black circles in all pictures represent a scale of 6.25 mm)

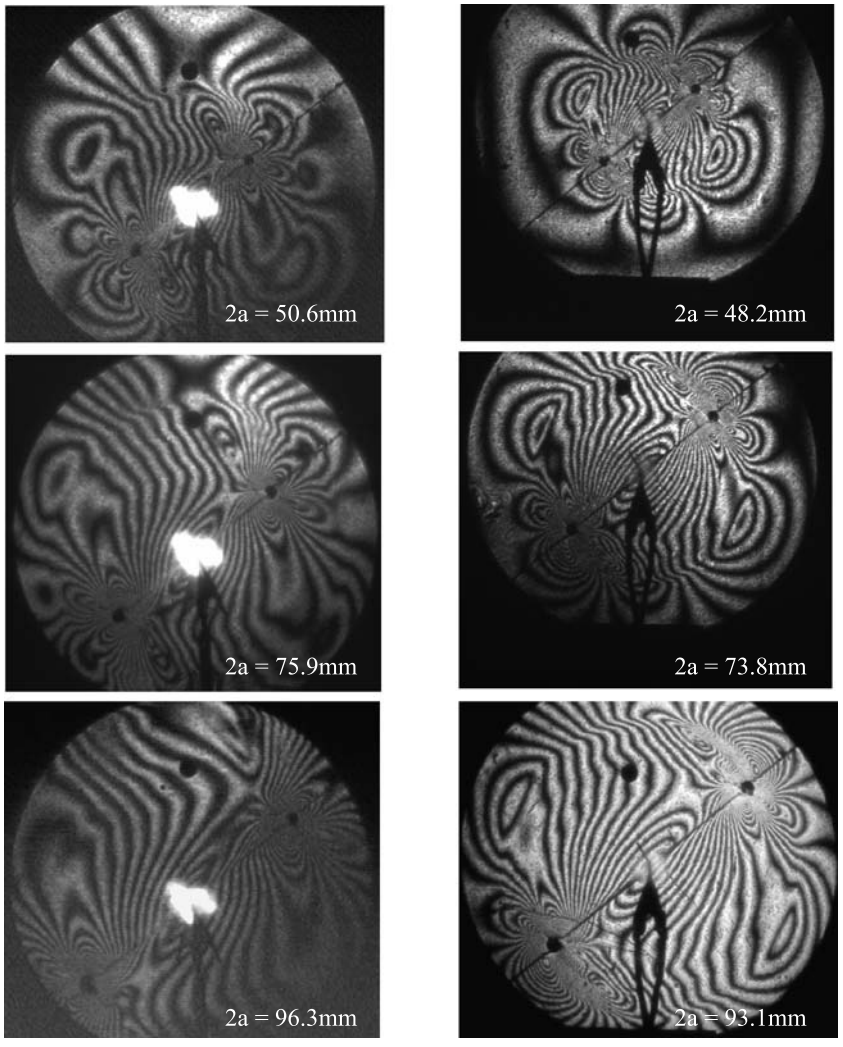

Fig. 4. Isochromatic fringes associated with two different adhesives of α = 40°: (**a**) "Strong" adhesive; (**b**) "Weak" adhesive

Accurate crack tip positions for the propagating cracks can be inferred by the location of small shadow spots corresponding to a traveling stress singularity as well as from the increased concentration of focused isochromatics at the crack tip. These are clearly visible in the figure. It can be observed from the fringes that for all three inclination angles as the crack length inreases, the size of the isochromatic loops and the number of fringes

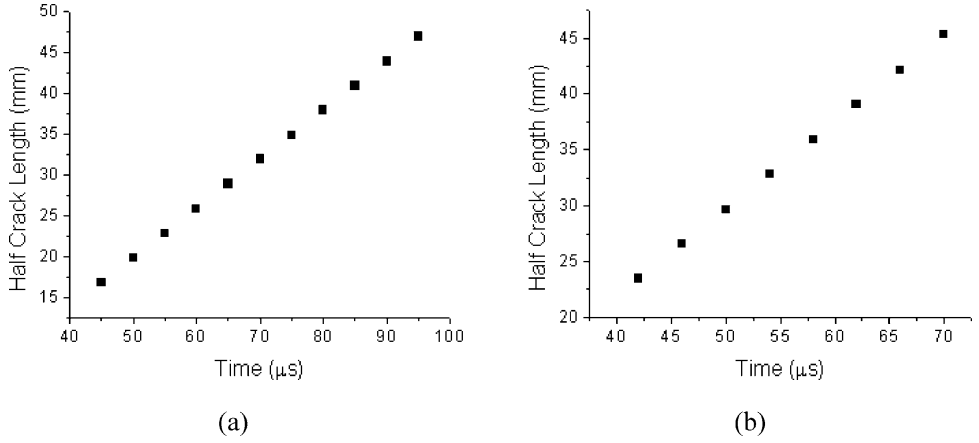

Fig. 5. Crack tip position history of two different adhesives of α = 40°: (**a**) "Strong" adhesive; (**b**) "Weak" adhesive

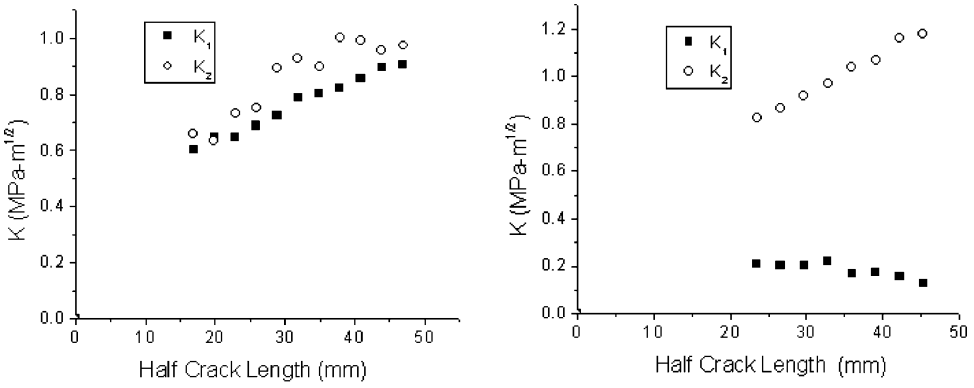

Fig. 6. Stress intensity factors history of two different adhesives of α = 40°: (**a**) "Strong" adhesive; (**b**) "Weak" adhesive

also increase around both crack tips. The increase in size and number of these fringes represent the increase in stress intensity around the crack tip. It can also be observed from Fig. 3 that the fringes are anti-symmetric with respect to crack nucleation point.

In the following sections, experiments of two different crack tip velocities for the geometry featuring, α = 40° are discussed. These velocities are achieved by changing the adhesive strength (toughness of the bond) while keeping the constant far-field tensile load of 8 MPa. Figure 4 displays the isochromatic fringe patterns at various crack lengths for these two different adhesives. These fringes are later analyzed to obtain crack tip position, crack velocity, and fracture parameters.

Crack Tip Position and Crack Velocity

The crack tip positions associated with the propagating crack tips are obtained from extrapolating to the center of the shadow spot surrounding each tip. The crack tip positions as a function of the time for two cases of α = 40°, and corresponding to a "strong" and a "weak" adhesives respectively are shown in Fig. 5(a) and 5(b). It can be seen from these figures that, the crack tip velocities for both cases are constant within the error of the experimental mea surement. The propagation velocity for the case of "strong" adhesive in Fig. 5(a) is approximately 600 m/s, for both crack tips. The propagation velocity for the "weak" adhesive specimen in Fig. 5(b) is approximately 790 m/s. It is important to mention here that the crack tips accelerate almost instantaneously to a constant velocity upon nucleation of the dynamic fracture event. We are not able to exactly quantify the acceleration phase because the crack tip location is obscured by the explosion plasma at the early stages of the event.

Dynamic Stress Intensity Factors and Energy Release Rate

Asymptotic crack tip stress fields for steady-state crack propagation [18] combined with the stress optic law, as

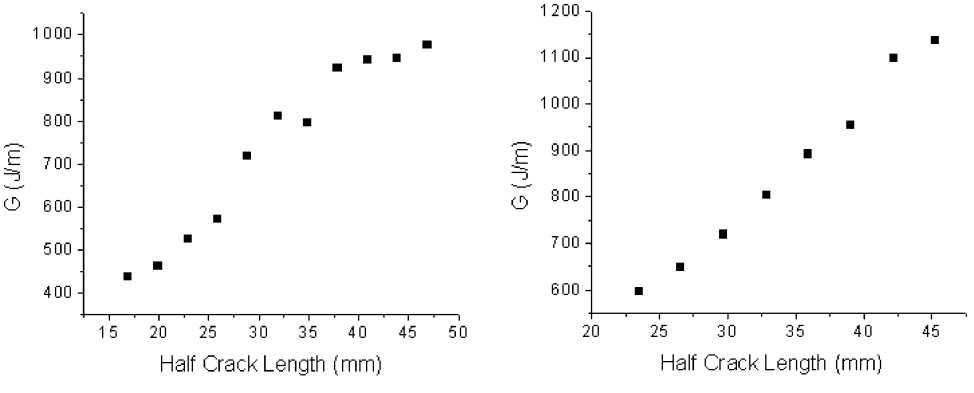

Fig. 7. Energy release rate history of two different adhesives of α = 40°: (**a**) "Strong" adhesive; (**b**) "Weak" adhesive

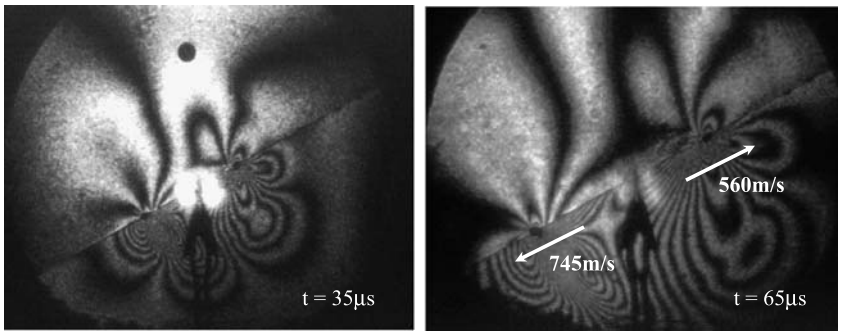

Fig. 8. Isochomatic fringes associated with crack propagation along the weak interface separating two dissimilar materials. Loss of anti-symmetry is visible

given below in the Eq. (1), define the isochromatics at a given point around the crack tip as follows:

$$\tau_{\max} = \frac{\sigma_1 - \sigma_2}{2} = \frac{Nf_\sigma}{2h} \tag{1}$$

In the above equation, τ_{max} is the maximum shear stress, σ_1 and σ_2 are maximum and minimum principal stresses respectively, N is the fringe order, f_σ is material fringe constant, and h is thickness of the specimen. The fringe orders of a selected set of points was be obtained from the photographs, and the dynamic mode-I and mode-II stress intensity factors, K_I^d and K_{II}^d, values were determined from these points using a non-linear least-squares method in conjunction with the Newton–Raphson technique [16].

The variation of dynamic mode-I and mode-II stress intensity factors histories as a function of the right hand crack tip position for both "strong" adhesive (crack velocity: 600 m/s or 62.5% of C_S of polycarbonate material) and "weak" adhesive (crack velocity: 790 m/s or 83% of C_S of polycarbonate material) are shown in the Fig. 6. It can be observed from the Fig. 6(a) that both mode-I and mode-II stress intensity factor values increase as the crack length increases. As discussed previously in the above sections, since the size of the isochromatic loops and number of fringes increase as the crack length increases, it can be expected that both mode-I and mode-II stress intensity factor values increase as the crack length increases. The average mode mixity [arc tan (K_{II}^d/K_I^d)] of the propagating crack associated with "strong" adhesive is around 48.24°. In case of crack propagation along the "weak" adhesive with a velocity of 790 m/s ($0.83C_s$ of polycarbonate material), mode-II stress intensity factor values are much higher than mode-I stress intensity factor values. The much higher values of mode-II values might be anticipated in advance if one observes the asymmetry of the fringe pattern implies highly predominantly shear crack propagation of high mode mixity as reported in case of crack propagation along bimaterial interfaces [19]. The average mode mixity [arc tan (K_{II}^d/K_I^d)] of the propagating crack associated with "weak" adhesive is around 79.3°.

The dynamic mode-I and mode-II stress intensity factors values as well as crack tip velocities are used to determine the dynamic energy release rate for

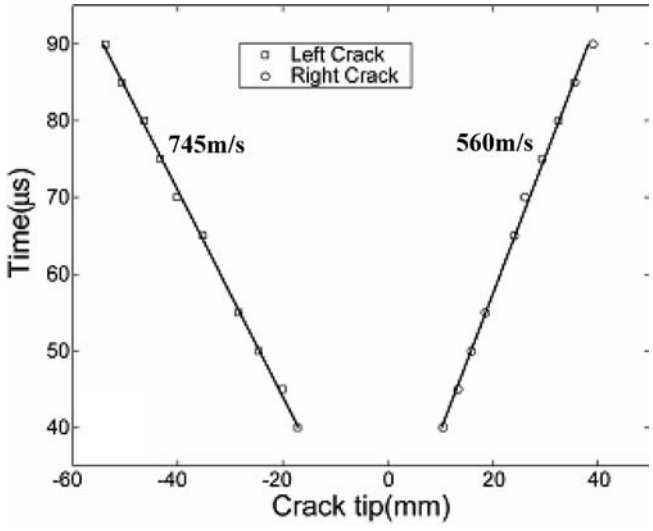

Fig. 9. Crack tip position history of both propagating crack tips in bonded dissimilar materials

both cases. The variation of energy release rate as a function of crack length is shown in the Fig. 7. For both cases, the dynamic energy release rate increases proportionately as the crack length. It implies that the interfacial resistance to spontaneous fracture propagation may not be a constant.

Experimental Results for Spontaneous Fracture in Dissimilar Materials

A preliminary experimental study has been conducted to study the spontaneous fracture and crack propagation along the weak bond separating two dissimilar materials. As discussed above, two different materials, Homalite-100 and polycarbonate are utilized and "weak" adhesive (HARDMAN epoxy) is used to bond these plates. As shown in Table 1, there is a 25% difference between the shear wave speeds of the two solids. Since both materials are photoelastic solids, isochromatic fringes can be seen from both halves of the specimen. Figure 8 shows the isochromatic fringes associated with a mixed-mode crack propagating along the bimaterial bond. The inclination angle is $\alpha = 30°$. The far-field tensile load applied in this case is 7 MPa. As clearly shown in the figure, the Homalite-100 half (upper half) has a considerably smaller number of fringes compared to the polycarbonate half (lower half). This is because the material fringe constant of Homalite-100 is almost three times higher than that of polycarbonate as given in Table 1. It can also be noticed from the figure that the stress field of the two crack tips is completely asymmetric with respect to the crack nucleation point. This is unlike the previous case of identical bonded plates where almost perfect anti-symmetry was observed. The shape and size of the resulting isochromatic fringes are different around the two crack tips. The crack tip positions associated with the propagating crack tips are obtained from extrapolating to the center of the shadow spot surrounding each tip. Figure 9 shows the crack tip position as a function of time for both crack tips. The left crack tip is propagating at constant velocity of 745 m/s, while the right crack tip is traveling at a constant velocity of 560 m/s. The crack velocity difference can be attributed to the fact that two crack tips propagate at opposite directions, to the directions of shearing of the more compliant of the two sides of the bimaterial combination. As a result of this, the sign of the vertical crack face displacements resulting because of the normal to shear coupling effects is opposite at the two tips. This is believed to retard or to enhance crack growth in a manner consistent to the experimental observations. Equivalent phenomena have been observed in relation to frictional interfacial crack under combined shear and compression [20] and dynamic shear rupture occurring along frictional interfaces separating Homalite-100 and Polycarbonate plates [21].

Conclusions

A novel experimental configuration has been designed to induce "spontaneous," mixed-mode fracture propagation along bonded similar and dissimilar plates. Two bond strengths have been considered. For similar bonded plates, the crack tip stress fields are anti-symmetric and the crack velocities are always found be sub-Rayleigh and constant within each experiment. These speeds are also the same for both crack tips. However the magnitude of these velocities varies with the strength of the adhesive and is a larger percentage of the Rayleigh wave speed as the bond strength decreases. The dynamic energy release rate is found to vary linearly with crack length. For dissimilar materials, the anti-symmetry of stress field and crack growth velocities are clearly broken.

Acknowledgments The authors would like to acknowledge the support of the Office of Naval Research (ONR) through grant number N00014-03-1-0435 (Dr. Y.D.S. Rajapakse, project monitor). Helpful discussions with Prof. G. Ravichandran from Caltech, with Prof. A. Shukla from University of Rhode Island and with Prof. L.B. Freund at Brown University are also acknowledged.

References

1. Ravichandar K, Knauss WG (1984) An experimental investigation into dynamic fracture .1. Crack initiation and arrest. Int J Fract 25(4):247–262.
2. Ravichandar K, Knauss WG (1984) An experimental investigation into dynamic fracture .4. On the interaction of stress waves with propagating cracks. Int J Fract 26(3):189–200.
3. Ravichandar K, Knauss WG (1984) An experimental investigation into dynamic fracture .3. On steady-state crack-propagation and crack branching. Int J Fract 26(2):141–154.
4. Ravichandar K, Knauss WG (1984) An experimental investigation into dynamic fracture .2. Microstructural aspects. Int J Fract 26(1):65–80.
5. Ravichandran G, Clifton RJ (1989) Dynamic fracture under plane-wave loading. Int J Fract 40(3):157–201.
6. Washabaugh PD, Knauss WG (1994) A reconciliation of dynamic crack velocity and Rayleigh-wave speed in isotropic brittle solids. Int J Fract 65(2):97–114.
7. Lambros J, Rosakis AJ (1995) Development of a dynamic decohesion criterion for subsonic fracture of the interface between two dissimilar materials. Proc R Soc Lond A451:711–736.
8. Lambros J, Rosakis AJ (1995) Dynamic decohesion of

bimaterials—Experimental-observations and failure criteria. Int J Solids Struct 32(17–18):2677–2702.
9. Rosakis AJ, Samudrala O, Singh RP, Shukla A (1998) Intersonic crack propagation in bimaterial systems. J Mech Phys Solids 46(10):1789–1813.
10. Singh RP, Lambros J, Shukla A, Rosakis AJ, (1997) Investigation of the mechanics of intersonic crack propagation along a bimaterial interface using coherent gradient sensing and photoelasticity. Proc R Soc Lond A453:2649–2667.
11. Coker D, Rosakis AJ, Needleman A (2003) Dynamic crack growth along a polymer-Homalite interface. J Mech Phys Solids 51(3):425–460.
12. Rosakis AJ, Samudrala O, Coker D (1999) Cracks faster than the shear wave speed. Science 284(5418):1337–1340.
13. Rosakis AJ (2002) Intersonic shear cracks and fault ruptures. Adv Phys 51(4):1189–1257.
14. Kavaturu M, Shukla A (1998) Opening-mode dominated crack growth along inclined interfaces: Experimental observations. Int J Solids Struct 35(30):3961–3975.
15. Kavaturu M, Shukla A (1999) Dynamic fracture of curved interfaces. Int J Fract 100(3):L3–L8.
16. Dally JW, Riley WF (1991) Experimental Stress Analysis. McGraw-Hill, New York.
17. Xia KW, Rosakis AJ, Kanamori H (2004) Laboratory earthquakes: The sub-Rayleigh-to-supershear rupture transition. Science 303(5665):1859–1861.
18. Liu C, Rosakis AJ (1994) On the higher-order asymptotic analysis of a nonuniformly propagating dynamic crack along an arbitrary path. J Elast 35(1–3):27–60.
19. Samudrala O, Rosakis AJ (2003) Effect of loading and geometry on the subsonic/intersonic transition of a bimaterial interface crack. Eng Fract Mech 70(2):309–337.
20. Qian W, Sun CT (1998) A frictional interfacial crack under combined shear and compression. Compos Sci Technol 58:1753–1761.
21. Xia KW, Rosakis AJ, Kanamori H, Rice JR (2005) Inhomogeneous faults hosting earthquakes in the laboratory: directionality and supershear. Science 308:681–684.